Simulation of Semiconductor Processes and Devices 2016
Edited by E. Bär, J. Lorenz, and P. Pichler

Automated source/mask/directed self-assembly optimization using a self-adaptive hierarchical modeling approach

Tim Fühner*, Przemysław Michalak*, Xiaofei Wu† and Andreas Erdmann*
* Fraunhofer Institute for Integrated Systems and Device Technology (IISB)
Schottkystrasse 10, 91058 Erlangen, Germany
tim.fuehner@iisb.fraunhofer.de
† Imaging Systems Laboratory, The University of Hong Kong,
Pokfulam, Hong Kong

***Abstract*—We propose an integrated approach to optimize lithography-generated guide structures for the directed self-assembly (DSA) of block co-polymers. Modeling the entire lithography/DSA co-process, little a priori knowledge is required, and well-performing solutions can be obtained quasi-automatically. To maintain a feasible optimization runtime, a reduced DSA model is employed. Predictivity and stability are ensured by the introduction of a self-adaptive calibration and model correction routine, for which a more exact phase-field DSA model is used. By an application to a via multiplication example, the feasibility and the potentials of the approach are demonstrated and discussed.**

I. Introduction

The directed self-assembly (DSA) of block copolymers (BCPs) holds the promise to extend the lifetime of nanolithography. It is considered a cost-efficient alternative to extreme ultra-violet lithography (EUVL) or pattern multiplication techniques. For the introduction of DSA as a lithography extension, its process steps must tightly integrate with the existing patterning process. Thus the compatibility of materials, processing times and machinery, but also of the employed metrology has to be ensured. Moreover, a computational infrastructure that reflects the requirement for an integrated process perspective has to be established. To this end, we have developed extensions to our computational lithography platform, Dr.LiTHO [1], that allow to seamlessly simulate the complete lithography/DSA co-process. Recently, we have demonstrated its potentials through a DSA-aware source/mask optimization method [2].

The progressive miniaturization of features implies an aggravated size and density constraint also of the vias, for example, for advanced SRAM circuits (for a simulation example, see [3]). Contact doubling is hence anticipated to become one of the first applications of DSA and is also aimed at in this work. The goal is to optimize the lithographic guide structure (Figure 1) such that it constitutes an ideal confinement for the double-cylinder DSA target. The simulation area $700 \cdot 250\,\mathrm{nm}^2$. The goal is to obtain

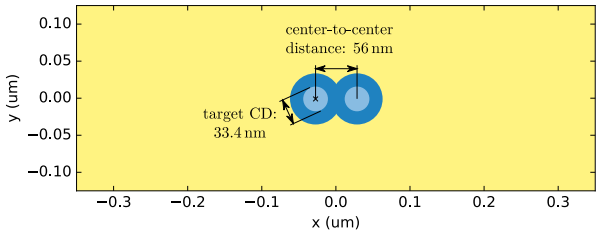

Fig. 1: The design target is a via multiplication, where each cylinder has a diameter of 33.4 nm and a position of ±28 nm. The simulation area is $700 \cdot 250\,\mathrm{nm}^2$.

two cylinders, each of which has a diameter of 33.4 nm and a center position at ±28 nm, respectively. A standard block copolymer (BCP)—Poly(styrene-*block*-methyl methacrylate) [PS-*b*-PMMA]—, with a PMMA volume fraction (f) of 0.31 and a segregation strength (χN) of 35, was supposed. Targeting at a two-phase configuration (PS-*b*-PMMA instead of the more common PMMA-*b*-PS-PS-*b*-PMMA case), the sidewalls are taken as PS-affine and the bottom as neutral. No pattern transfer, neither hard mask nor PMMA etch, are taken into account. As figures of merit, standard lithographic metrics such as the maximization of the common process window are used. To retain a feasible runtime, we have employed a simulation approach, termed the interface Hamiltonian (IH) model, of the block copolymers [4], [5], in which the phase interface location is inferred from the free energy minimization problem in the strong segregation limit. With the proposed procedure, we are able to generate ideal guide patterns without the provision of any a priori information.

II. Simulation and Optimization Setup

The optimization is performed with an evolutionary algorithm. One iteration consists of concurrent evaluations of several candidate solutions. The computation routine

978-1-5090-0818-6/16/$31.00

for each candidate can be summarized as follows:[1] (1) The topological mask according to the mask optimization variables is generated, and the spectra are computed using the Waveguide method. Additionally, the mask manufacturability penalty is determined. (2) A process window evaluation is conducted. The bulk image and the resist profile are computed. For the resist simulation, a three-dimensional compact model, called *"RoadRunner,"* is used [6]. (3) For the two-dimensional interface Hamiltonian (IH) approach, a footprint is extracted from the three-dimensional resist profile. For that purpose, the average of a fifth of the resist layers starting from the bottom (at ten percent of the total height) is computed and the contour at the develop time of 60 s is extracted. (4) Since the employed module makes use of a polar Legendre polynomial representation, an according fit, yielding the respective coefficients, is performed. (5) The so-obtained coefficients are used as the input for the subsequent free-energy minimization step, during which the interface of the inner cylinder is inferred. (6) Both the CD and the placement error are measured independently in x and y direction. (7) The CD is measured independently in x and y direction, giving rise to two process windows whose overlap is to be maximized. (8) Similarly, the placement error is evaluated and used as a minimization criterion.

III. Self-adaptive Model Correction

The model employed approximates the interfacial behavior between the two polymers. Specifically in limiting situations such as non-ideal confinements, this may lead to an inexact prediction of placement and CDs. More severely, it may result in a false estimation of the separation of the two inner cylinders. A respective situation is shown in Figure 2, where the IH model result is compared with the more exact Ohta-Kawasaki (OK) phase-field model[7]. Despite a close similarity of the guide structures, the OK model result shows a separation of both cylinders only in one of the cases. By contrast, the interface Hamiltonian model predicts separated cylinders in both cases. Since the OK model accounts for the interfacial behavior between the two polymers, its result can be expected to better reflect the actual situation.

To improve the placement prediction and to distinguish non-stable configurations, we have included a self-adaptive model correction stage, using the Ohta-Kawasaki model, into our optimization strategy.

The flow (Figure 3) can be summarized as follows: (a) Using a multi-objective evolutionary algorithm, the process window of the multiplied cylinders is maximized. Sidelobes, placement errors and mask manufacturability constraints are included as additional figures of merit. The evaluation (b) is performed based on the measurements

[1]For all simulations, a 193-nm immersion scanner and a standard (non-calibrated) resist are assumed. The models are part of the Fraunhofer IISB simulator *Dr.LiTHO* [1] and its recent DSA extension *Dr.Seal*.

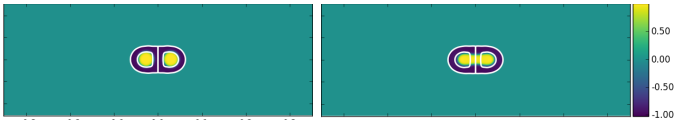

(a) (b)

Fig. 2: Similar guide pattern solutions leading to different configuration predictions after DSA. The interface Hamiltonian result is depicted as a white contour laid over the phase distribution computed by the OK model (-1 denotes the majority, 1 the minority phase). (a) Both models predict a separation of the cylinders, whereas in (b) the OK model results in one blended, deformed structure.

after the DSA, which is simulated using the IH approximation. The resulted CD and placement values are corrected by applying according offset factors that are retrieved from a database (c), which is updated from the occasionally conducted OK correction step. Initially, the database is empty, and hence the unmodified IH results are used. Each set of correction factors in the eventually growing database corresponds to a confinement topology. Three solutions with the most similar confinement compared with the IH candidate are retrieved from the database. The correction for CDs and placement is then applied as a weighted average of these three neighbors. The weights are proportionate to the distance from the actual confinement. Formally, we have

$$x^*_{C_t} := x_{C_t} + \frac{1}{3}\sum_i (1 - d(C_t, C_i))o_{C_i}, \qquad (1)$$

where x denotes the respective value of interest (CDs and placement values for both cylinders and in both directions) obtained with the IH model for the target confinement (C_t). The correction stage (e) is triggered after a predefined number (e.g., ten) of iterations. There, from the pool of candidates yielded by the optimizer (d), those solutions that are underrepresented in the database—that is, those candidates that exhibit the least similarity with any solution stored in the database—are selected. The ratio of verified solutions is set to five to ten percent of the candidate pool size. To limit the runtime, it should not become to large; large enough, however, to account for representative results. The selected solutions are evaluated using the OK model. The differences between these result and the original IH predictions are taken as the correction factors. They are stored in the database alongside with the confinement representation. Afterward, all solutions in the candidate pool are updated according to the new database status.

IV. Results

In a first step, we have generated the correction database using candidate solutions obtained from our previous optimization study [2]. For that purpose, we have stored the

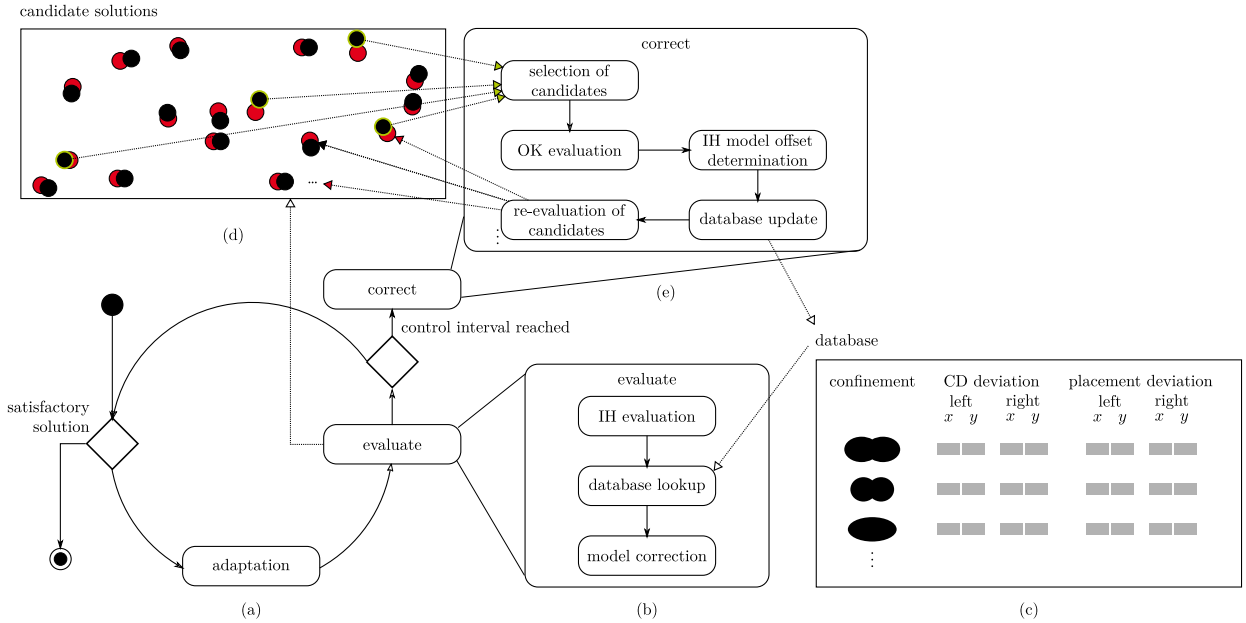

Fig. 3: Optimization flow with self-adaptive model correction.

contours of the guide structures along with the CD and placement values resulted from the OK model. To study the impact of the correction approach, we have performed a cross-validation procedure. We have re-evaluated candidate solutions from the same optimization run as before that have not been accounted for in the course of generating the correction database. Figure 4(a) shows the process window of a well-performing candidate solution obtained with the proposed optimization routine without model correction. The usable process window, resulting from the overlapping ±10-percent tolerance region of the CDs measured in x and y direction, exhibits a depth-of-focus (DOF) of about 72 nm and an exposure latitude (EL) of about 5 %. The re-evaluation using the correction database and the approach described in the previous section, gives rise to a slightly different process window with a DOF of about 68 nm and an EL of almost 6 % (Figure 4(b)). The CD deviation from the interface Hamiltonian and the OK model was slightly decreased from −0.82 nm (x) and 0.69 nm (y) to −0.75 nm (x) and 0.47 nm (y). The placement error difference was reduced from 1.8 nm to 1.6 nm. On average of all cross-validated solutions, the deviation between the OK model and the IH model was decreased by around 10 %.

As a next step, we have conducted a new optimization with the parameters and objectives but using the correction database and routine. That is, for each evaluation step, the interface Hamiltonian results were adjusted according the stored OK results. A champion solution is shown in Figure 5. The candidate shows an ample process window, which was improved in comparison with the former optimization study. The dose latitude is 9.4 %, and the depth-of-focus is about 80 nm.

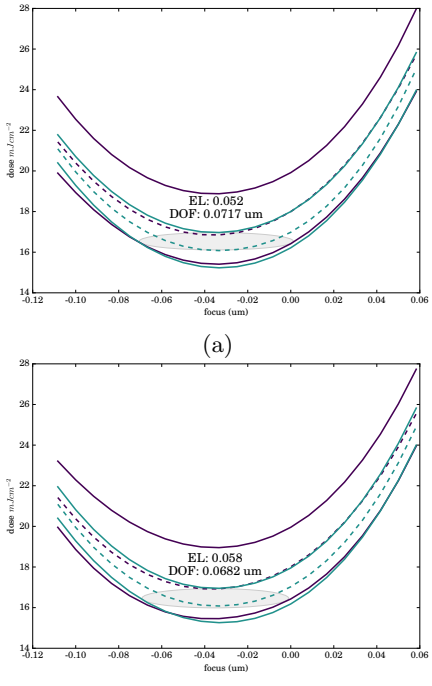

Fig. 4: Comparison of process windows obtained with (a) the non-corrected and (b) the corrected IH model.

To evaluate the overall improvement of the corrected IH model in comparison to the uncorrected one, we have evaluated the CD and placement deviations between the models of all champion solutions after the final iteration. More specifically, we have computed the difference between the exact OK model verification result and that of

the corrected IH model, and compared it to the difference of the OK model with the uncorrected IH model. On average, an improvement—that is, a reduction of the difference—of about 0.02 nm in x and 0.15 nm in the y direction was achieved for the CD values. The maximum improvement was 0.3 nm and 0.7 nm, respectively. The mean placement error improvement for the x direction was 0.28 nm, and the respective maximum was 0.53 nm. No improvement of the placement error in the y direction can be observed. Also the OK model predicts only marginal y-placement errors, which can be attributed to the fact that the block copolymer is tightly confined in this direction.

The decrease in CD and placement error differences but also the improved result compared with the former optimization study are indicative for the viability of the approach. To further decrease the error of the IH model, further studies on the influential factors of the correction approach are necessary. Specifically, the interval between calibration stages and the weight factor of the correction term, which influences how aggressively the IH model result is adjusted, need to be investigated.

V. Conclusions

We have proposed an integrated source/mask/DSA optimization approach, which we have demonstrated through a contact hole multiplication example using a grapho-epitaxy guide pattern. With the provision of only little a priori knowledge, ample usable process windows with minimal placement errors were achieved. To maintain a feasible runtime, a reduced DSA model was employed. This model is well-suited to broadly estimate CDs and placement errors of the vias. Especially under limiting conditions such as non-ideal confinements, however, more rigorous models are required for an exact prediction. To this end, we have devised an integrated calibration technique, which uses a phase-field model to correct the approximated results. The corrections are applied for each evaluation step in the optimization loop. We have shown how this adaptive correction technique increases the predictive power of the evaluation step and hence leads to an increase in accuracy of the optimization results. Future work will be directed toward a tighter coupling of the calibration and the optimization stages, a study on the calibration intervals and the correction weight factors, and an application of the proposed approach to other patterns including lines and spaces.

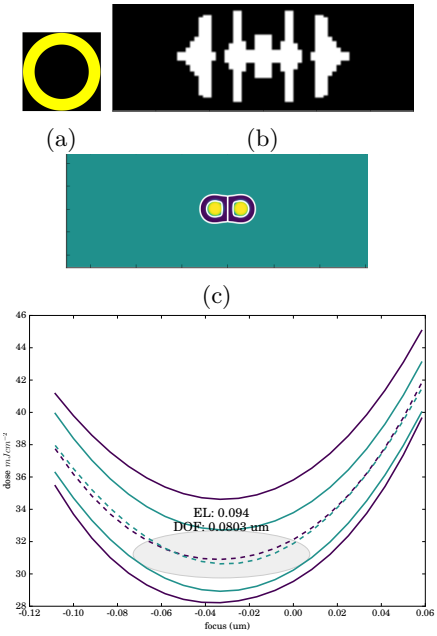

	x	y
non-corrected IH model		
CD	34.1 nm	34.8 nm
deviation from OK solution	0.27 nm	0.25 nm
placement error	−0.8 nm	0 nm
deviation from OK solution	0.63 nm	0 nm
corrected IH model		
CD	34 nm	34.7 nm
deviation from OK solution	0.15 nm	0.29 nm
placement error	−0.4 nm	0 nm
deviation from OK solution	0.29 nm	0 nm

(e)

Fig. 5: Champion solution of the correction-enabled optimization: (a) illumination source, (b) photomask, (c) profile after DSA; the contour (white) obtained with the interface Hamiltonian model is laid over the OK verification result, (d) usable process window resulting from the overlap of measurements in x and y direction; (e) corrected and non-corrected CD and placement values.

Acknowledgments

The research leading to these results has received funding from the European Union Seventh Framework Programme (FP7/2007–2013) under grant agreement no. 619793 CoLiSA.MMP.

References

[1] T. Fühner, T. Schnattinger, G. Ardelean, and A. Erdmann, "Dr.LiTHO: a development and research lithography simulator," in *Proc. SPIE*, 2007, p. 65203F.

[2] T. Fühner, P. Michalak, U. Welling, J. C. Orozco-Rey, M. Müller, and A. Erdmann, "An integrated source/mask/DSA optimization approach," in *Proc. SPIE*, 2016, p. 97800M.

[3] E. Bär, A. Burenkov, P. Evanschitzky, and J. Lorenz, "Simulation of process variations in FinFET transistor patterning," in *SISPAD*, 2016, submitted.

[4] U. Welling, W. Li, J. O. Rey, P. Michalak, T. Fühner, A. Erdmann, and M. Müller, "Reduced models for dsa simulations," in *13th Fraunhofer IISB Lithography Simulation Workshop*, Behringersmühle, Germany, 2015.

[5] P. D. Olmsted and S. T. Milner, "Strong segregation theory of bicontinuous phases in block copolymers," *Macromolecules*, vol. 31, no. 12, pp. 4011–4022.

[6] D. Flagello, R. Matsui, K. Yano, and T. Matsuyama, "The development of a fast physical photoresist model for OPE and SMO applications from an optical engineering perspective," in *Proc. SPIE*, 2012, p. 83260R.

[7] T. Ohta and K. Kawasaki, "Equilibrium morphology of block copolymer melts," *Macromolecules*, vol. 19, pp. 2621–2632, 1986.